Open access • Journal Article • DOI:10.1103/PHYSREVB.74.081101

Understanding mixed valent materials : Effects of dynamical core-hole screening in high-pressure x-ray spectroscopy — Source link

Claudia Dallera, Ola Wessely, Massimiliano Colarieti-Tosti, Olle Eriksson ...+8 more authors

Institutions: Polytechnic University of Milan, Uppsala University, Linköping University, Radboud University Nijmegen ...+3 more institutions

Published on: 21 Aug 2006 - Physical Review B (American Physical Society)

Topics: Valence (chemistry) and Valency

PHYSICAL REVIEW B **74**, 081101(R) (2006)

Understanding mixed valent materials: Effects of dynamical core-hole screening in high-pressure x-ray spectroscopy

C. Dallera,[1] O. Wessely,[2] M. Colarieti-Tosti,[3] O. Eriksson,[2] R. Ahuja,[2] B. Johansson,[2] M. I. Katsnelson,[4] E. Annese,[5] J.-P. Rueff,[6,*] G. Vankó,[7] L. Braicovich,[1] and M. Grioni[8]

[1]*INFM—Dipartimento di Fisica, Politecnico di Milano, piazza L. da Vinci 32, 20133 Milano, Italy*

[2]*Department of Physics, Uppsala University, Box 530, Uppsala, Sweden*

[3]*Department of Physics, Chemistry and Biology, Linköping University, 581 83 Linköping, Sweden*

[4]*Institute for Molecules and Materials, Radboud University of Nijmegen, NL-6525 ED Nijmegen, The Netherlands*

[5]*INFM—Dipartimento di Fisica, Università degli Studi di Modena e Reggio Emilia, via Campi 213/A, I-41100 Modena, Italy*

[6]*Synchrotron SOLEIL, L'Orme des Merisiers, Saint-Aubin Boîte Postale 48, 91192 Gif-sur-Yvette, France*

[7]*European Synchrotron Radiation Facility, Boîte Postale 220, 38043 Grenoble Cédex, France*

[8]*IPN, Ecole Polytechnique Fédérale (EPFL), CH-1015 Lausanne, Switzerland*

(Received 30 June 2006; published 21 August 2006)

Changes in the electronic structure of Yb, a material whose valence is modified under pressure, are observed with remarkable detail in x-ray absorption and emission data measured between ambient conditions and 20 GPa. These changes are reproduced by a theory that essentially does not rely on experimental parameters, and includes dynamical core-hole screening. From the combined experimental and theoretical data we can firmly establish on a quantitative level how the valency of an intermediate valence material is modified by pressure. In metallic Yb it increases from 2 to 2.55±0.05 between 0 and 20 GPa.

DOI: 10.1103/PhysRevB.74.081101 PACS number(s): 71.28.+d, 71.15.−m, 78.70.En

A crucial aspect of materials with incomplete $4f$ or $5f$ shells is the valency. It is the central parameter in understanding heavy-fermion materials, anomalous superconductors, and obviously intermediate valent (IV) materials.[1,2] In the series of the rare-earth metals, Yb and Eu show a number of anomalous properties (like large equilibrium volume) demonstrating their divalent ground state, in contrast to the prevailing trivalent behavior of the rest of this group of elements. The valency in, e.g., metallic Yb reflects a balance between the energy required to excite a $4f$ electron into the valence band from the $4f^{14}(sd)^2$ (Yb^{2+}) ground state, and the larger cohesive energy of the $4f^{13}(sd)^3$ (Yb^{3+}) configuration. This balance may be altered by applying external pressure.

The relative stability of the Yb^{2+} and Yb^{3+} ionic configurations, and the possibility of a valence transition under pressure, were already discussed in Ref. 3. More recently, it has been shown that the equation of state of Yb under high pressure can be described very accurately by an *ab initio* calculation for the IV state, the Coulomb interaction between $4f$ electrons and $5d$ holes being of crucial importance.[4,5] From the experimental side, the anomalous compressibility of Yb, which is intermediate between divalent Ca and trivalent Lu,[6] suggests a continuous valence transition to a fully trivalent state above 100 GPa.[7] However, it has turned out to be difficult to experimentally verify this on a microscopic scale.

The Yb valence is more directly probed by x-ray absorption spectroscopy (XAS) at the Yb L_3 edge ($2p^64f^N+h\nu_{in} \rightarrow 2p^54f^N\varepsilon d$; εd is an electron in the d continuum).[8,9] Pioneering XAS experiments, which indeed measured pressure-dependent spectral changes,[10] were hindered by the strong absorption in the pressure cell, and by a large spectral broadening ($\Delta E \sim 5.3$ eV) due to the short lifetime of the deep $2p$ core hole. More accurate experiments are now enabled by advances in x-ray spectroscopy, and by the improved brilliance of modern synchrotron sources. We have here utilized this fact to obtain precise information on the evolution of the electronic configuration of ytterbium. In the experiment the radiative $L\alpha_1$ deexcitation of the XAS final state ($2p^64f^N+h\nu_{in} \rightarrow 2p^54f^N\varepsilon d \rightarrow 2p^63d^{\emptyset}4f^N\varepsilon d+h\nu_{out}$) was explored. Since the energy broadening ($\Delta E \sim 0.6$ eV) is determined by the longer lifetime of the $3d$ hole, this process gives access to finer spectral details.[11] The corresponding spectral function $I(h\nu_{in},h\nu_{out})$ can be sampled in one-dimensional scans where either $h\nu_{out}$ or $h\nu_{in}$ is fixed, corresponding to "high-resolution" partial fluorescence yield XAS (PFY XAS) or $L\alpha_1$ resonant inelastic x-ray scattering (RIXS) spectra, respectively. RIXS is especially powerful because the contribution of each electronic configuration in the ground state ($4f^{13}$ or $4f^{14}$ for Yb) can be selectively enhanced by tuning $h\nu_{in}$ to specific energies along the absorption edge.[12]

We performed high-pressure experiments at beamline ID16 of the European Synchrotron Radiation Facility (Grenoble, France), which provides a focused (130×50 μm^2) monochromatic x-ray beam at the sample position. The sample, a 25-μm-thick ytterbium foil (from Goodfellow), was loaded in a diamond anvil cell, using high-strength Be as gasketing material and ethanol as pressure-transmitting medium. Pressure could be measured *in situ* by the conventional ruby fluorescence technique. Both the incident and the emitted radiation passed through the Be gasket in the horizontal scattering plane, to avoid strong absorption by the diamonds. X rays emitted at 90° from the incident beam were analyzed using the (620) Bragg reflection of a 1-m-radius spherically bent silicon crystal, and then detected by a Peltier-cooled Si diode. We measured PFY XAS spectra by scanning the incident energy through the Yb L_3 edge ($h\nu_{in} \sim 8.95$ keV) while recording the intensity of the emitted characteristic Yb $L\alpha_1$ fluorescence ($h\nu_0 = 7.415$ keV). RIXS spectra were recorded for selected values of $h\nu_{in}$ across the L_3 edge. The overall energy resolution was ~1.5 eV. Depending on the incident photon energy the acquisition time per RIXS spectrum varied between ~15 and 45 mins.

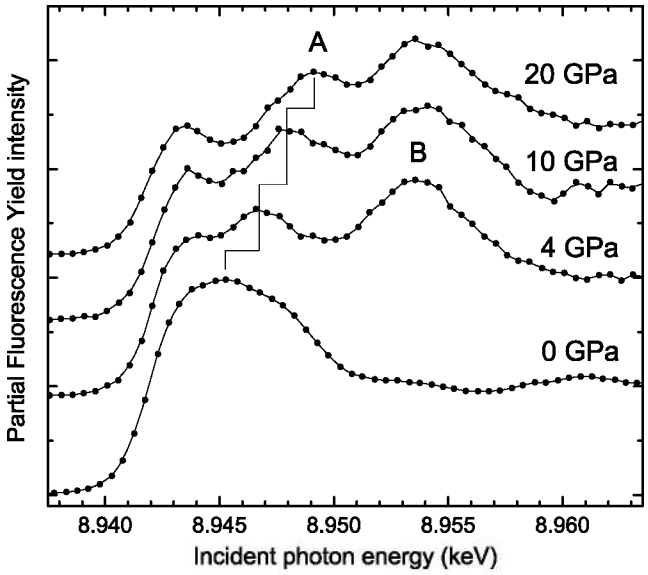

FIG. 1. $L\alpha_1$ PFY XAS spectra of Yb at selected pressures.

PFY XAS data measured at pressures between 0 and 20 GPa are shown in Fig. 1. The broad line shape at ambient pressure is indicative of underlying structure that could not be appreciated in lower-resolution data.[10] With increasing pressure, spectral weight is transferred from threshold to a new peak B at ~10 eV higher energy. Moreover, an intermediate peak A emerges from the broad threshold, and progressively drifts to higher energy. Changes are already quite visible at 4 GPa, the boundary between the Yb fcc and bcc phases. For a pure Yb^{2+} or Yb^{3+} ground state, due to dipole selection rules, the Yb L_3 XAS spectrum is proportional to an unoccupied density of states (DOS) of d symmetry, modulated by matrix elements and distorted by the attractive core-hole potential.[13] In IV Yb compounds, the line shape is interpreted as the superposition of two replicas of the d DOS, weighted by the ground state weights $w(2+)$ and $w(3+)$ of the Yb^{2+} and Yb^{3+} configurations, and offset by several eV's. The replicas correspond to $2p^54f^{14}\varepsilon d$ and $2p^54f^{13}\varepsilon d$ final states, and their energy separation reflects the large Coulomb repulsion between the $2p$ and $4f$ holes.[14] Therefore the observed spectral weight transfer indicates an increasing Yb^{3+} weight in the hybrid ground state, in agreement with Ref. 10. The added element in the data of Fig. 1 is feature A, which changes with pressure and suggests that the d DOS is modified as a function of this parameter. A closer analysis (see below) substantiates this interpretation.

Figure 2(a) shows the series of RIXS spectra measured through the L_3 edge at 20 GPa. They are plotted as a function of the energy transfer $E_T=h\nu_{in}-h\nu_{out}$. Spectral features whose energy tracks with $h\nu_{in}$, in the Raman regime, appear at constant energy transfer. The Raman feature final states at ~1.526 and ~1.536 keV (indicated by the arrows) originate from the Yb^{2+} and Yb^{3+} ground state configurations. The dispersive peak (marked by the asterisk) observed at larger incident energies is the characteristic $L\alpha_1$ fluorescence, whose intensity follows the XAS profile. The 20 GPa RIXS spectra for all incident energies can be consistently decomposed, following the guidelines described in Ref. 12, to yield

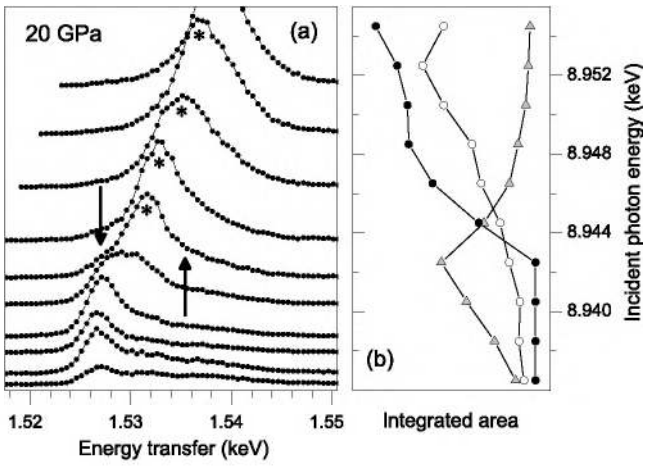

FIG. 2. (a) RIXS spectra of Yb measured through the L_3 edge at 20 GPa, as a function of the energy transfer $E_T=h\nu_{in}-h\nu_{out}$ (the lower two spectra multiplied by 2). The incident energy $h\nu_{in}$ is increasing in 2 eV steps, from 8.936 keV (bottom spectrum) to 8.954 keV (top spectrum). The vertical arrows indicate the Raman signatures of the Yb^{2+} and Yb^{3+} configurations, respectively, at ~1.526 and ~1.536 keV. The dispersing peak marked by an asterisk is the $L\alpha_1$ fluorescence. (b) Intensity profiles obtained from a decomposition of the spectra of the left panel. Triangles, Yb^{2+}; empty circles, Yb^{3+}; filled circles, fluorescence.

the intensity profiles of Yb^{2+} and Yb^{3+} and of the $L\alpha_1$ fluorescence [Fig. 2(b)]. Their energy dependence enables a qualitative interpretation of the PFY XAS spectra of Fig. 1: the Yb^{2+} signal dominates near threshold (and peaks at $h\nu_{in}$=8.942 keV), while the Yb^{3+} intensity peaks at ~10 eV higher energy. The decomposition of the 4 and 10 GPa RIXS data leads to the same conclusion. At 0 GPa the spectra were fitted only with 2+ and fluorescence signals. Changes in the RIXS line shape with pressure are illustrated in Fig. 3(a) for the representative value $h\nu_{in}$=8.942 keV, at the Yb^{2+} resonance. We decomposed the 20 GPa spectrum into separate Yb^{2+} and Yb^{3+} contributions. The former is a rescaled replica of the ambient pressure line shape.

The Yb valence can be deduced at all pressures from the relative intensities of the Yb^{2+} and Yb^{3+} RIXS components, as $v=2+w(3+)/[w(2+)+w(3+)]$: the experimental weights $w(2+)$ and $w(3+)$ are obtained as the maximum values of their respective intensity profiles. The result of this analysis [Fig. 3(b)] shows that the Yb valence increases from 2 to 2.55 ± 0.05 between ambient pressure and 20 GPa. The error bars account for statistical errors, for corrections associated with the energy dependence of the penetration length, and for uncertainties in the precise resonance energy.

A theoretical description of the observed spectroscopic changes must go beyond standard ground state electronic structure theory, which is based on the local density approximation (or gradient corrected functionals): these calculations do not always reproduce well experimental data, which arise from a combination of the initial and final densities of states.[15,16] The method presented here accounts for the superposition of initial and final electronic states and applies to many complex systems. In general, dynamical screening of the core hole created in the excitation process is expected to

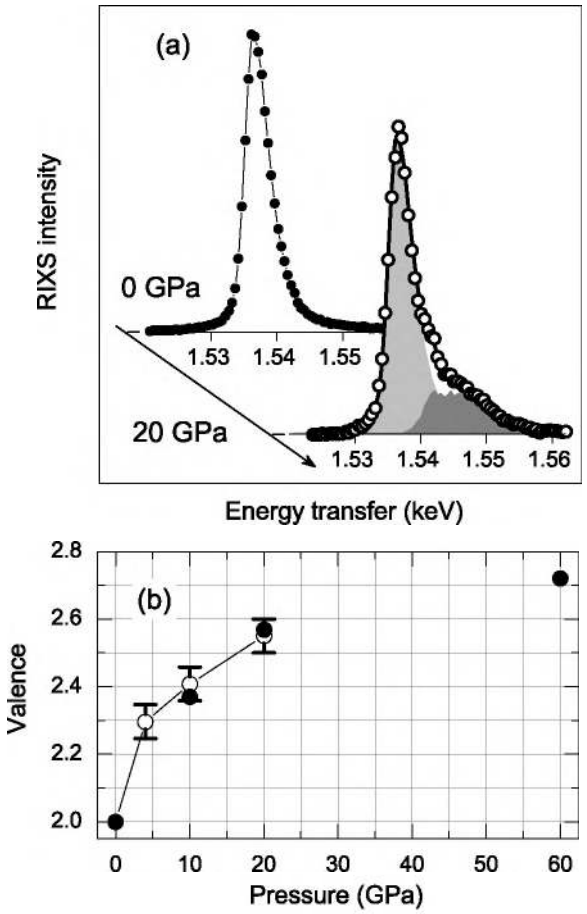

FIG. 3. (a) $L\alpha_1$ RIXS spectra ($h\nu_{in}$=8.942 keV) of Yb measured at ambient pressure (filled connected dots) and 20 GPa (hollow dots). The thick continuous line at 20 GPa is the sum of a scaled replica of the 0 GPa line shape representing the Yb^{2+} component (light gray area) and of an Yb^{3+} component (dark gray area). The latter is obtained as the difference between the measured spectrum and the Yb^{2+} component. (b) Values of the Yb valency determined from the RIXS data (filled dots) and from our first-principles calculation (white dots). Experimental and theoretical values coincide at 0 GPa.

play an important role. A solution to this arduous theoretical problem may be obtained by the first-principles multiband version[16] of the Mahan–Nozières–De Dominicis (MND) theory.[17–19] A further complication arises for mixed valent materials, namely, that the spectral weights of the divalent and trivalent contributions must be evaluated. We have solved this part of the problem by calculating, for each pressure, the ground state weights $w(2+)$ and $w(3+)$ using the mean-field description of the Kimball-Falicov model, where the *d-f* Coulomb interaction plays an important role.[20] These weights are compared to experiment in Fig. 3(b), and we note that the agreement between theory and experiment is very good. We remark that all parameters in the Kimball-Falicov model (the energy difference between di- and trivalent configurations, the Falicov interaction parameter, the renormalized Fermi energy, and the *spd-f* hybridization matrix element) were calculated from first principles.

The XA spectrum was calculated as described below. The initial and final state Yb^{2+} and Yb^{3+} Green's functions were calculated from first principles. A relative offset of 10 eV was applied to the Green's functions to reproduce the energy separation of the Yb^{2+} and Yb^{3+} core level binding energies (the calculated value for this energy splitting was 8.2 eV). We then computed a complete solution of the dynamical screening problem[16] for Yb^{2+} and Yb^{3+}, where the initial and final state Green's functions play a crucial role. The XA spectrum of the mixed valence compound was obtained by multiplying the Yb^{2+} and Yb^{3+} spectra with the theoretical weights $w(2+)$ and $w(3+)$.

The first-principles calculations were done using the plane-wave VASP code[23,24] within the projector augmented wave[25] method. The exchange-correlation energy was described by the Ceperley and Alder functional[26] parametrized by Perdew and Zunger.[27] The mixed valency of Yb was modeled using supercells containing Yb atoms with three and two valence electrons. For the calculation at 10 GPa a cell with 10 Yb^{2+} and 6 Yb^{3+} atoms was used, to simulate a valency close to that determined by the Kimball-Falicov model.[20] For the same reason, in the calculation at 20 GPa a cell with seven Yb^{2+} and nine Yb^{3+} was used. The Green's functions were calculated for the Yb^{2+} and Yb^{3+} atoms with a set of neighboring atoms representing the mixed valent alloy.

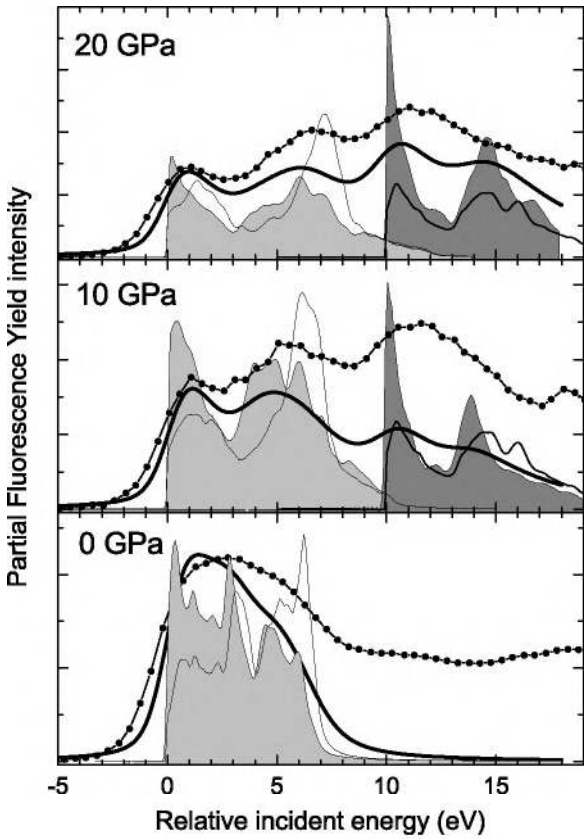

FIG. 4. Comparison of experimental PFY XAS spectra of metallic Yb at selected pressures (dotted lines) with calculation: shaded curves are the unbroadened Yb^{2+} (light gray) and Yb^{3+} (dark gray) XAS spectra calculated by the MND theory as described in the text. Thick lines represent the broadened sum of the latter curves. Also shown for comparison are the initial state local density approximation density of states (thin lines).

The Monkhorst-Pack scheme[28] was applied with $5\times5\times5$ and $3\times3\times3$ k-point meshes, and a kinetic energy cutoff at ~200 eV was used for the plane-wave basis set. In order to simulate a system with a core excitation we adopted the $Z+1$ approximation for the excited atom of our supercells. Finally, we added a Lorentzian broadening, whose fulll width at half maximum (FWHM) was taken to increase linearly above threshold to account for the final state lifetime:[21] $\Delta E(\mathrm{FWHM})=0.6+0.15(E-E_{threshold})$ eV. In order to compare the theoretical spectra with experiment, we introduced a Gaussian experimental broadening $\Delta E(\mathrm{FWHM})=1.5$ eV. No phenomenological background was added to the calculated spectra.

A comparison of experimental and calculated spectra for 0, 10, and 20 GPa (Fig. 4) reveals an overall good agreement. The calculated features above 10 eV from the Fermi edge are partially obscured by the large spectral broadening and by the experimental background (not included in the calculation). The comparison provides an interpretation of the observed energy shift of feature A: it reflects the increasing separation with pressure between the center of mass of the unoccupied d DOS of the 2+ configuration and the Fermi energy. The reason for this is an increasing overlap between the wave functions of the d orbitals with increasing pressure and decreasing lattice constant. The result is a broadening of the d band and a corresponding shift of the spectral features. Also shown in Fig. 4 is the initial state local density approximation DOS, showing modestly good agreement with the data. The final state DOS (not shown here) is quite similar to the MND data. It should be noted that this finding is far from being a standard result of MND theory since the core-hole valence-electron interaction is known in many cases to produce an "edge singularity," with an associated increase of the XAS intensity at the threshold energy: in a recent work[16] it was shown that the relative intensities between various features of the XAS spectrum of graphite were significantly different in the MND calculation compared to a final state calculation.

The development in experimental capabilities in combination with advancements in the theoretical description of mixed valent materials is shown here to yield a remarkably detailed description of ground and excited state properties. The most noticeable property is the valency, recently discussed, e.g., by Strange *et al.*,[22] that we now can monitor at a very detailed level as a function of pressure. Our theory reproduces the observations quite accurately. The excited state properties are revealed by the PFY XAS signal and also here theory and experiment agree well. The combined PFY XAS and RIXS data, and the comparison with theory, yield very detailed information on how the valency of a material changes with applied pressure. The method is an important development for our understanding of mixed valent materials in general.

We thank A. Shukla for his help in the preparatory phase of the experiment and M. Mattesini for valuable discussions in the early stages of this work. We acknowledge financial support from the Göran Gustafsson Foundation, the Swedish Natural Science Council, and the Center for Dynamical Processes, Uppsala University. Work in Lausanne is supported by the Swiss National Science Foundation.

*Permanent address: Laboratoire de Chimie Physique—Matière et Rayonnement (UMR 7614), Université Pierre et Marie Curie, 11 rue P. et M. Curie, F-75231 Paris Cedex 05, France.

[1] R. D. Parks, *Valence Instabilities and Narrow Band Phenomena* (Plenum Press, New York, 1977).
[2] J. M. Lawrence, P. S. Riseborough, and R. D. Parks, Rep. Prog. Phys. **44**, 1 (1981).
[3] B. Johansson and A. Rosengren, Phys. Rev. B **11**, 2836 (1975).
[4] A. Delin, L. Fast, B. Johansson, J. M. Wills, and O. Eriksson, Phys. Rev. Lett. **79**, 4637 (1997).
[5] M. Colarieti-Tosti, M. I. Katsnelson, M. Mattesini, S. I. Simak, R. Ahuja, B. Johansson, C. Dallera, and O. Eriksson, Phys. Rev. Lett. **93**, 096403 (2004).
[6] K. Takemura and K. Syassen, J. Phys. F: Met. Phys. **15**, 543 (1985).
[7] G. N. Chesnut and Y. K. Vohra, Phys. Rev. Lett. **82**, 1712 (1999).
[8] A. Kotani, T. Jo, and J. C. Parlebas, Adv. Phys. **37**, 37 (1988).
[9] D. Malterre, Phys. Rev. B **43**, 1391 (1991).
[10] K. Syassen, G. Wortmann, J. Feldhaus, K. H. Frank, and G. Kaindl, Phys. Rev. B **26**, R4745 (1982).
[11] K. Hämäläinen, D. P. Siddons, J. B. Hastings, and L. E. Berman, Phys. Rev. Lett. **67**, 2850 (1991).
[12] C. Dallera, E. Annese, J. P. Rueff, A. Palenzona, G. Vankó, L. Braicovich, A. Shukla, and M. Grioni, Phys. Rev. B **68**, 245114 (2003).
[13] U. von Barth and G. Grossmann, Phys. Scr. **21**, 580 (1980).
[14] J. M. Lawrence, G. H. Kwei, P. C. Canfield, J. G. DeWitt, and A. C. Lawson, Phys. Rev. B **49**, 1627 (1994).
[15] O. Wessely, P. Roy, D. Åberg, C. Andersson, S. Edvardsson, O. Karis, B. Sanyal, P. Svedlindh, M. I. Katsnelson, R. Gunnarsson, D. Arvanitis, O. Bengone, and O. Eriksson, Phys. Rev. B **68**, 235109 (2003).
[16] O. Wessely, M. I. Katsnelson, and O. Eriksson, Phys. Rev. Lett. **94**, 167401 (2005).
[17] G. D. Mahan, *Many-Particle Physics* (Plenum Press, New York, 1990), Chap. 8.
[18] P. Nozières and C. T. De Dominicis, Phys. Rev. **178**, 1097 (1969).
[19] V. I. Grebennikov, Yu. A. Babanov, and O. B. Sokolov, Phys. Status Solidi B **79**, 423 (1977).
[20] V. Yu. Irkhin and M. I. Katsnelson, Sov. Phys. JETP **63**, 631 (1986).
[21] M. Grioni, J. F. van Acker, M. T. Czyzyk, and J. C. Fuggle, Phys. Rev. B **45**, 3309 (1992).
[22] P. Strange, A. Svane, W. H. Temmerman, Z. Szotek, and H. Winter, Nature (London) **399**, 756 (1999).
[23] G. Kresse and J. Hafner, Phys. Rev. B **47**, R558 (1993).
[24] G. Kresse and J. Furthmüller, Phys. Rev. B **54**, 11169 (1996).
[25] P. E. Blochl, Phys. Rev. B **50**, 17953 (1994).
[26] D. M. Ceperley and B. J. Alder, Phys. Rev. Lett. **45**, 566 (1980).
[27] J. P. Perdew and A. Zunger, Phys. Rev. B **23**, 5048 (1981).
[28] H. J. Monkhorst and J. D. Pack, Phys. Rev. B **13**, 5188 (1976).